Published in final edited form as:
Pharm Res. 2014 April ; 31(4): 1046–1058. doi:10.1007/s11095-013-1226-x.

Ocular Delivery of pRNA Nanoparticles: Distribution and Clearance After Subconjunctival Injection

Liang Feng,
Division of Pharmaceutical Sciences, James L. Winkle College of Pharmacy, University of Cincinnati, 3225 Eden Avenue 136 HPB, Cincinnati, Ohio 45267, USA

S. Kevin Li,
Division of Pharmaceutical Sciences, James L. Winkle College of Pharmacy, University of Cincinnati, 3225 Eden Avenue 136 HPB, Cincinnati, Ohio 45267, USA

Hongshan Liu,
Department of Ophthalmology, College of Medicine, University of Cincinnati, Cincinnati, Ohio 45267, USA

Chia-Yang Liu,
Department of Ophthalmology, College of Medicine, University of Cincinnati, Cincinnati, Ohio 45267, USA

Kathleen LaSance,
Vontz Core Imaging Laboratory (VCIL), University of Cincinnati, Cincinnati, Ohio 45267, USA

Farzin Haque,
Department of Pharmaceutical Sciences, School of Pharmacy and Markey Cancer Center, University of Kentucky, Lexington, Kentucky 40536, USA

Dan Shu, and
Department of Pharmaceutical Sciences, School of Pharmacy and Markey Cancer Center, University of Kentucky, Lexington, Kentucky 40536, USA

Peixuan Guo
Department of Pharmaceutical Sciences, School of Pharmacy and Markey Cancer Center, University of Kentucky, Lexington, Kentucky 40536, USA

S. Kevin Li: likv@uc.edu

Abstract

Purpose—RNA nanoparticles derived from the three-way junction (3WJ) of the pRNA of bacteriophage phi29 DNA packaging motor were previously found to be thermodynamically stable. As the nanoparticles could have potential in ocular drug delivery, the objectives in the present study were to investigate the distribution of pRNA nanoparticles after subconjunctival injection and examine the feasibility to deliver the nanoparticles to the cells of cornea and retina.

Correspondence to: S. Kevin Li, likv@uc.edu.

Methods—Alexa647-labeled pRNA nanoparticles (pRNA-3WJ and pRNA-X) and double-stranded RNA (dsRNA) were administered *via* subconjunctival injection in mice. Alexa647 dye was a control. Topical administration was performed for comparison. Ocular clearance of pRNA nanoparticles and dsRNA after the injection was assessed using whole-body fluorescence imaging of the eyes. The numbers of cells in the ocular tissues with nanoparticle cell internalization were determined in fluorescence microscopy of dissected eye tissues.

Results—After subconjunctival injection, pRNA nanoparticles and dsRNA were observed to distribute into the eyes and cleared through the lymph. pRNA-3WJ, pRNA-X, and dsRNA were found in the cells of the conjunctiva, cornea, and sclera, but only pRNA-X was in the cells of the retina. Topical administration was not effective in delivering the nanoparticles to the eye.

Conclusions—The pRNA nanoparticles were delivered to the cells in the eye *via* subconjunctival injection, and cell internalization was achieved in the cornea with pRNA-3WJ and pRNA-X and in the retina with pRNA-X. Only the X-shape pRNA-X could enter the retina.

Keywords

double-stranded RNA; ocular delivery; pRNA nanoparticle; subconjunctival; topical

Introduction

Recent advances in drug discovery have provided a number of novel macromolecules such as oligonucleotides, aptamers, and anti-VEGF monoclonal antibodies and their fragments for the treatment of ocular diseases (1,2). Approved oligonucleotide-based therapies include fomivirsen (Vitravene®) for the treatment of cytomegalovirus retinitis (3) and pegaptanib (Macugen®) for wet age-related macular degeneration (4). An anti-platelet derived growth factor DNA aptamer (Fovista™) is also in clinical trials in a combined therapy to treat choroidal neovascularization (5). For chronic treatments, the conventional routes of systemic administration and intravitreal injection are either not effective or have drawbacks. Systemic administration is not effective due to the blood-retina barrier and is not preferred because of potential systemic toxicity. Intravitreal injection is related to potential side effects such as intraocular bleeding, ocular hypertension, infection, and retinal detachment, and repeated injections significantly increase these risks (6). Therefore, there is an unmet need of a more effective method to deliver new therapeutic agents such as oligonucleotides to the eye, especially to the posterior segment of the eye.

The concept of RNA nanotechnology first proven 15 years ago (7) has recently generated a strong interest in the scientific community, as evidenced by a surge in the number of publications over the last 5 years (8,9). RNA has the simplicity in design with the characteristics of DNA and can be manipulated to provide functions similar to some proteins (8). RNA-based therapeutic agents include small interfering RNA (siRNA), ribozymes, RNA aptamers, and miRNAs. In spite of the uniqueness of RNA-based therapies, a major problem in RNA nanotechnology is that RNA molecules are relatively unstable, especially at ultra-low concentration after administration into the body. Another major concern is the susceptibility of RNA to RNase degradation in the serum or in the body. Simple chemical modifications such as incorporation of 2′-Fluoro (2′-F) nucleotides can make the RNA

resistant to degradation, while retaining biological activity (10–12). Recently, an RNA three-way junction (3WJ) motif from the pRNA of bacteriophage phi29 DNA packaging motor was discovered to be thermodynamically and chemically stable (Fig. 1a). It was resistant to 8-M urea denaturation and remained intact at ultra-low concentrations (10,12). The pRNA-3WJ motif was extended to a four-way X-shaped nanoparticle, denoted pRNA-X, exhibiting similar robust properties (10) (Fig. 1b). These pRNA nanoparticles can be modified to harbor multiple modules with different functionalities such as RNA aptamer, reporter moiety, and therapeutic siRNA or miRNA as their subunits all in the same single nanoparticle. Due to these advantages, the development of efficient and specific pRNA nanoparticles can provide unique opportunities for the treatment of ocular diseases.

Effective drug delivery to the eye in the treatment of ocular diseases depends on reliable pharmacokinetic data and the understanding of drug delivery and clearance mechanisms in the eye. Ocular pharmacokinetic studies have provided useful information on the distribution of drugs in the eye and in the development of novel drug delivery methods. In addition to conventional pharmacokinetic approaches of tissue dissection, methods such as microdialysis (13), fluorophotometry (14), and magnetic resonance imaging (MRI) (15) have been used in the studies of ocular pharmacokinetics and to determine the routes of drug delivery and clearance after periocular, intrascleral, and intravitreal administration. Despite these recent efforts in studying the mechanisms and pharmacokinetics of ocular drug delivery, the distribution and clearance after ocular drug delivery are still difficult to predict (16). This is partly due to the complicated anatomy and physiology of the eye. Particularly, ocular pharmacokinetics of macromolecules such as pRNA nanoparticles and their distribution and clearance after periocular administration are not well understood.

The objectives of the present study were to (a) determine the ocular distribution of Alexa647-labeled pRNA nanoparticles (pRNA-3WJ and pRNA-X) after subconjunctival injection and (b) examine the feasibility to deliver the nanoparticles to the cells of the cornea and retina. Topical administration was evaluated for comparison. Whole-body fluorescence imaging of the eyes and fluorescence microscopy of dissected ocular tissues were performed. In the whole-body imaging study, pRNA nanoparticles were injected subconjunctivally in mice, and the distribution and clearance of the nanoparticles in the eyes were monitored *in vivo*. In the microscopy study, the eyes of the animals were enucleated at predetermined time points after subconjunctival injection or topical administration, then the eyes were dissected, and the delivery of the pRNA nanoparticles to the ocular tissues was assessed using grid projection fluorescence microscopy. Alexa647-labeled dsRNA and Alexa647 dye were also used and served as references in the present study.

Materials and Methods

Animals

Female mice (7–10 weeks old, SKH1 and C57BL/6 strains) were supplied from Charles River Laboratories International (Wilmington, MA). All experiments were conducted in compliance with the Association for Research in Vision and Ophthalmology (ARVO) Statement for the Use of Animals in Ophthalmic and Vision Research and with approval of

the Institutional Animal Care and Use Committee (IACUC) at the University of Cincinnati (Cincinnati, OH).

Materials

The pRNA nanoparticles, Alexa647-labeled pRNA-3WJ and pRNA-X, were synthesized from RNA fragments (Trilink) according to the procedure described previously (10,12). The RNA nanoparticles contained 2′-F U and C nucleotides to make them resistant to RNase degradation. Alexa647-labeled dsRNA of 16 bp was synthesized using the same procedure. Alexa647 was purchased from Life Technologies Corp. (Grand Island, NY). Phosphate-buffered saline (PBS, pH 7.4, consisting of 0.01 M phosphate buffer, 0.0027 M potassium chloride, and 0.137 M sodium chloride) was prepared by dissolving PBS tablets (Sigma-Aldrich, St. Louis, MO) in distilled, deionized water and filtered with 0.22 μm filter for sterilization. The pRNA and dsRNA suspensions and Alexa647 solution were prepared by diluting 100 μM pRNA, dsRNA, and Alexa647 (in diethylpyrocarbonate treated water) with PBS at 1:1 (v/v) right before the experiments. Paraformaldehyde (PFA) solution 4% (w/v) was prepared by diluting 16% (w/v) PFA solution (EM grade, Electron Microscopy Sciences, Hatfield, PA) in PBS. 4′,6-Diamidino-2-phenylindole dihydrochloride (DAPI) was purchased from Sigma-Aldrich (St Louis, MO). Xylazine and ketamine were purchased from Phoenix Pharmaceuticals (St. Joseph, MO).

Subconjunctival Injection and Topical Administration

For the subconjunctival injection, the mice were anesthetized by intraperitoneal (*i.p.*) injection of 10 mg/kg xylazine and 80 mg/kg ketamine. Then, the conjunctiva was gently pulled from the sclera with a pair of forceps, and 10 μL of pRNA or dsRNA suspension were injected into the superior subconjunctival region using a microsyringe with a 33G needle. Alexa647 solution serving as a reference for comparison was injected subconjunctivally using the same method.

Topical administration study of pRNA nanoparticles, dsRNA, and Alexa647 was also performed in mice to compare with the subconjunctival injection. The mice were anesthetized using the same method, and then 10 μL of the pRNA or dsRNA suspensions or Alexa647 solution were directly applied as eyedrops on the ocular surface.

Whole-Body Fluorescence Imaging

Whole-body fluorescence imaging study was performed after subconjunctival injection on SKH1 mice. The mice were anesthetized with 2% isoflurane during the imaging. The ocular surface and surrounding area were cleaned with saline before the first imaging to ensure that there was no significant contamination from the residues from the dosing. On a few occasions, cleaning of the eye was repeated after an imaging scan and the animal was imaged again for comparison to validate the cleaning procedure. Fluorescence images were acquired using Bruker *In-vivo* Multispectral Imaging System FX (MS FX Pro) with Carestream Molecular Imaging (MI) software version 5.0.7.24 (Rochester, NY) that was capable of multi-spectral fluorescence, X-ray, and surface optical imaging. Two imaging protocols were used: imaging of the whole body (at normal resolution) and of the eye (at higher resolution). The whole body was imaged using fluorescence imaging parameters of

630 nm (excitation) and 700 nm (emission), field of view (FOV) of 120 mm, f-stop of 2.51, 4×4 pixel binning, and exposure time of 1 s. The eye (at higher resolution) was imaged using the same fluorescence imaging parameters except with FOV of 22 mm, 1×1 pixel binning, and exposure time of 5 s. In the experiments, a small centrifuge vial of known concentration of Alexa647 was used as a reference standard and imaged with the animals. For anatomical reference, X-ray (exposure time of 30 s) and surface optical imaging (exposure time of 0.175 s) with the same FOV as the fluorescence imaging were used. To monitor ocular clearance of the pRNA nanoparticles, dsRNA, and Alexa647, fluorescence imaging was performed at predetermined time points (e.g., 0.5, 1, 2, 4, 6, 7.5, and 9.5 h) after the injection. After each imaging scan, the animals were returned to their cages. In a separate experiment, 6.25 nM to 0.4 μM of the pRNA nanoparticles, dsRNA, and Alexa647 in PBS were prepared in centrifuge vials and imaged using the same fluorescence imaging protocol to determine the fluorescence intensity *vs.* concentration relationships for comparison.

In the post processing analyses, the fluorescence images were overlaid on corresponding anatomical reference images and manual region of interest (ROI) method was used to calculate the mean fluorescence intensities of the ROI at different time points.

Fluorescence Microscopy

Fluorescence microscopy study was performed after subconjunctival injection and topical administration on C57BL/6 mice. The mice were sacrificed by cervical dislocation under anesthesia at 6, 12, and 20 h after subconjunctival injection and 12 h after topical administration. The eyes including the conjunctiva and eyelids were collected and washed (by soaking) in PBS for 2×30 min at room temperature to remove blood and other contaminations.

Immediately after enucleation of the eyes and washing, the eyes were fixed on a piece of wax in 4% PFA solution for 2 h at 4°C to ensure that the conjunctivas were flattened. Then, the eyes were rinsed with PBS for 2×10 min and dissected. Tissues of conjunctiva, cornea, retina, and sclera were isolated and stained with 0.01% DAPI solution overnight at room temperature. After DAPI staining, the tissues were rinsed with PBS for 3×10 min and mounted on a microscopy slide with Mowoil (PVA). Grid projection microscopy (apotome fluorescence microscopy) was performed using Carl Zeiss AxioCam Observer Z1 microscope coupled with AxioVision SE64 Rel. 4.8 analytical system (Carl Zeiss Microscopy, LLC, Thornwood, NY). Tissues were imaged at the wavelengths of 461 nm (for the cell nucleus stained by DAPI) and 665 nm (for the Alexa647 marker). Images were analyzed by counting the numbers of cells with the cell nucleus surrounded by or overlapped with Alexa647 signals (i.e., cell internalization of pRNA nanoparticles or dsRNA) in 0.42 mm×0.33 mm FOV at the same imaging plane in the tissues.

To investigate the delivery of pRNA nanoparticles and dsRNA to the contralateral eyes, subconjunctival injection was performed as described in the “Subconjunctival Injection and Topical Administration” section. At 20 h after the injection, the mice were sacrificed and the contralateral eyes were collected and treated as described above.

Possible effects of contamination of pRNA nanoparticles and dsRNA, such as those remaining on the skin around the eyes after dosing, upon the microscopy results were investigated. In this assessment, blank eyes were collected following the normal procedures as described above except that 1 μL of pRNA or dsRNA suspension (one-tenth of the amount injected subconjunctivally) was added into the PBS solution with the eye during the 30-min initial wash to simulate the pRNA and dsRNA residues after dosing.

Statistical Analysis

All experiments were performed at least in triplicate, except for the contralateral eye evaluation and the contamination assessment in the microscopy study which were in duplicate. Results were expressed as the mean±standard deviation (SD) and compared using ANOVA tandem Newman-keuls test (*q* test). Differences between the groups were considered as significant at $p < 0.05$.

Results

Whole-Body Fluorescence Imaging

Figure 2 shows the representative whole body images of the animals after subconjunctival injection. The mean fluorescence intensities at the eyes and cervical lymph nodes are summarized in Fig. 3. For comparison, Fig. 3a presents the relationships between the fluorescence intensities of pRNA nanoparticles, dsRNA, and Alexa647 and their concentrations in PBS in centrifuge vials. The fluorescence intensities of pRNA-X, pRNA-3WJ, dsRNA, and Alexa647 all increased linearly with their respective concentrations in PBS with Alexa647 having the highest apparent quantum yield in aqueous solution. In this experiment and in the whole-body imaging experiments, it was also noted that no significant day-to-day variability of the fluorescence intensities of these vials was observed over the duration of the present study.

In the whole body images, the mean intensities at the eyes decreased rapidly after the injection of pRNA nanoparticles, dsRNA, and Alexa647, indicating fast clearance at the site of injection and in the eye (Fig. 3). Alexa647 had the fastest clearance that its mean intensity decreased to the background noise level at approximately 4.5 h after the injection. The mean intensities of pRNA nanoparticles and dsRNA decreased to the background level at approximately 6 to 9 h after the injection. There was no detectable fluorescence signal at the contralateral eyes in the entire study.

For the cervical lymph nodes, fluorescence signals were detected at the homolateral lymph nodes and not the contralateral lymph nodes after subconjunctival injection of pRNA nanoparticles and dsRNA (Fig. 2). The presence of pRNA in the cervical lymph node was verified in a separate study that imaged the cervical lymph node after the dissection and isolation of the tissue from the animal following subconjunctival injection. From the trends in Fig. 3, the mean intensities of the lymph nodes correspond to the mean intensities at the eyes, indicating that the lymphatic circulation is a major clearance route for the pRNA nanoparticles and dsRNA after subconjunctival injection. In contrast, no signal was detected in the cervical lymph nodes after subconjunctival injection of Alexa647 (Fig. 2). It should be

noted that the concentration of the pRNA nanoparticles, dsRNA, and Alexa647 in the eyes and lymph nodes cannot be quantified from the intensity *vs.* concentration relationships in Fig. 3a due to the different microenvironments of the fluorophore in tissues and solution.

Figure 4 shows the representative fluorescence images of the eye after subconjunctival injection of pRNA-X. Note that the fluorescence intensities of the images of the eyes are different from those of the whole body in Fig. 2 due to the different parameters of the fluorescence imaging protocols. The images show the delivery of the pRNA nanoparticle into the eye from the injection site over time. Similar distribution patterns of fluorescence signals were also observed for pRNA-3WJ and dsRNA. For example, approximately 2 h after the injection, strong fluorescence signals were observed at the injection site and around the eye compared to those at the eye (Fig. 4a). The fluorescence signals then spread into the eye and the surrounding area at approximately 4 h after the injection (Fig. 4b). In contrast, after subconjunctival injection of Alexa647, the signal remained primarily at the injection site, indicating less effective ocular delivery (data not shown). Although the fluorescence images in these experiments provide evidence that the pRNA nanoparticles and dsRNA were distributed into the eye after subconjunctival injection, the exact locations of the tissues emitting the fluorescence signals could not be determined due to the limitations of this method. Whole-mount fluorescence microscopy study was therefore performed to investigate this question in the present study.

pRNA Nanoparticles in Conjunctiva After Subconjunctival Injection

Figure 5 shows the representative microscopy images of the conjunctiva after subconjunctival injection in the microscopy study. Significant internalization of pRNA nanoparticles and dsRNA in the cells of the conjunctiva was observed. The numbers of cells in the conjunctiva with the internalization of pRNA nanoparticles and dsRNA at 6 h, 12 h, and 20 h are summarized in Fig. 6. The figure shows a significant number of cells with pRNA and dsRNA internalization in the superior conjunctiva near the injection site at 6 h after the injection and the number decreases at 12 h and 20 h. In contrast to the superior conjunctiva, the inferior conjunctiva had significantly lower numbers of cells with pRNA and dsRNA internalization ($p < 0.05$). For Alexa647, no fluorescence signal of the dye was found in the cells after subconjunctival injection.

pRNA Nanoparticles in Cornea After Subconjunctival Injection

Figures 7 and 8 show the representative microscopy images of the cornea after subconjunctival injection. Significant internalization of pRNA nanoparticles and dsRNA in the cells of the cornea was observed. The numbers of cells in the cornea with pRNA and dsRNA internalization at 6 h, 12 h, and 20 h are summarized in Fig. 9. At 6 h after subconjunctival injection, the delivery of pRNA nanoparticles to the cells of the cornea was attained. Although the numbers of cells with nanoparticle internalization decreased over time from 6 h to 20 h, significant numbers of nanoparticles were retained in the cells up to 20 h. The data also show similar clearance among the pRNA nanoparticles and dsRNA under the conditions in the present study. For Alexa647, no cell internalization was observed in the cornea after the injection.

pRNA Nanoparticles in Sclera and Retina After Subconjunctival Injection

Representative microscopy images of the retina and sclera after subconjunctival injection are shown in Figs. 10 and 11, respectively. Figure 12 presents the numbers of cells with pRNA and dsRNA internalization in the retina and sclera after the injection. Different from the results of conjunctiva and cornea, only pRNA-X was found in the cells of the retina at 6 h after the injection. The number of cells in the retina with pRNA-X internalization decreased rapidly and no nanoparticle was present in the retina at 12 h after the injection. In the sclera, cell internalization of pRNA nanoparticles and dsRNA was observed with pRNA-X demonstrated the fastest distribution to and clearance in the cells of the sclera among the RNA systems studied ($p < 0.05$). Similar to the results of the conjunctiva and cornea, no Alexa647 was found in the retina and sclera after subconjunctival injection.

Ocular Delivery After Topical Administration

No pRNA nanoparticles and dsRNA were found in the cells of conjunctiva, cornea, retina, and sclera at 12 h after topical eyedrop administration. This suggests that topical administration was not an effective ocular delivery method for both pRNA and dsRNA compared with subconjunctival injection.

Delivery to Contralateral Eye

At 20 h after subconjunctival injection, no pRNA nanoparticles and dsRNA were found in the cells of the contralateral eyes, indicating that the pRNA nanoparticles and dsRNA were not delivered into the contralateral eyes. This is consistent with the results in the present whole-body imaging study.

Microscopy Study Contamination Assessment

In the examination of the effects of possible contamination of pRNA and dsRNA in the fluorescence microscopy study, some fluorescent spots (possibly due to the contamination) could be found in the conjunctiva and sclera, but no overlapping of cell nucleus and Alexa647 signals was observed. This is evidence that the pRNA and dsRNA residues around the eyes after dosing did not affect the results of the microscopy study.

Discussion

Ocular Delivery of pRNA Nanoparticles

Topical administration for drug delivery to the posterior segment of the eye is generally considered to be ineffective due to precorneal clearance, ocular tissue barriers such as cornea and conjunctiva, long diffusional pathway from the anterior segment to the back of the eye, and clearance in the eye (6). Topical administration is also ineffective for the delivery of macromolecules to the anterior segment of the eye because macromolecules cannot penetrate intact cornea effectively (17). Periocular injections are better methods for ocular delivery of macromolecules (18), and intravitreal injection is required for effective delivery to the posterior segment of the eye (6,19). An advantage of periocular injections is that they are less invasive than intravitreal injection. Among the periocular injection

methods, subconjunctival injection has been a recent interest due to its ability to utilize the transscleral route.

In the present study, both pRNA nanoparticles and dsRNA were delivered to the cells of the cornea after subconjunctival injection. This is consistent with the results in a previous subconjunctival injection study of bevacizumab, a monoclonal antibody drug. In this previous study, within 6 h after the injection, bevacizumab was detected in the cornea close to the injection site and spread to other parts of the cornea at later time points (20). This suggests that the subconjunctival route can be effective in the delivery of macromolecules to the cornea and is relatively nonspecific.

For nanoparticle delivery to the retina, the successful delivery of pRNA-X into the cells of the retina after subconjunctival injection is significant despite the short retention time of the nanoparticle in the cells of the retina. Although targeted delivery and cell internalization of nanoparticles/macromolecules in the retina have been observed in previous studies, they were achieved by more invasive methods. For example, intravitreal injection of polylactide (PLA) and poly (lactide-co-glycolide) (PLGA) nanoparticles was used in the delivery of fluorochromes and fluorescent protein plasmids to the retinal pigment epithelium (RPE) (21,22). Iontophoresis and intravitreal injection were used to deliver single-stranded oligonucleotide for targeted gene repair in the retina (23). Different from these methods, the internalization of pRNA-X in the cells of retina in the present study provides an opportunity for cell transfection and targeted gene delivery to the retina *via* simple subconjunctival injection.

The mechanism of pRNA-X delivery to the cells of retina after subconjunctival injection is not clear, but a combination of factors such as RNA stability, tissue barrier permeability, and cell uptake efficiency may be involved. RNA stability is probably not the only factor because pRNA-3WJ is as stable as pRNA-X but was not detected in the retina after subconjunctival injection. The different results of pRNA-X and pRNA-3WJ suggest that the delivery is nanoparticle specific, probably related to the size and shape of the nano-particle. From a diffusion perspective, Alexa647 with its small molecular size (molecular weight ∼1,300 Da) compared to the nanoparticles should have the fastest diffusion and penetration rates across the transscleral barrier, but no Alexa647 was found in the retina after subconjunctival injection in the present study. For transscleral delivery *via* subconjunctival injection, although the sclera can be viewed as a porous membrane with effective pore radius in the order of 20 nm (24,25) and allows the permeation of macromolecules, the RPE is considered to be a barrier for the penetration of polar molecules and macromolecules (26). Previous studies have suggested that some macromolecules such as full-length ovalbumin can diffuse through RPE (27). It is therefore possible that pRNA nanoparticles of specific sizes and shapes can penetrate the RPE barrier and reach the retina after subconjunctival injection. The different result of pRNA-X from those of Alexa647, pRNA-3WJ, and dsRNA suggests that the successful delivery of pRNA-X into the cells of retina is not due to a single factor. Future studies are needed to determine the exact mechanism of how pRNA-X is delivered into the cells of retina after subconjunctival injection.

Clearance of pRNA Nanoparticles After Subconjuntival Injection

The clearance of drugs in the subconjunctival space after subconjunctival injection is generally fast (28–31). For small molecules, their half-lives in the subconjunctival space are in the order of 10–40 min. The main mechanisms of ocular clearance following subconjunctival injection are lymphatic and blood clearance in the periocular space (29,32,33). In the present study, pRNA nanoparticles were distributed from the injection sites to different ocular tissues (conjunctiva, cornea, retina, and sclera) and then cleared from the eyes rapidly. Particularly, the fluorescence intensities at the eyes decreased quickly that no signal was detected at 9 h after the injection in the whole-body imaging study. The lymph circulation was found to be involved in ocular clearance of the pRNA nanoparticles and dsRNA as evidence by the fluorescence signals at the cervical lymph nodes. This is consistent with the previous findings of subconjunctival clearance of small molecules and macromolecules (29,32,33). However, no lymphatic clearance through the cervical lymph nodes was observed in the present study with Alexa647 (the control). This suggests a potential difference between the extent of lymphatic clearance of the pRNA nanoparticles and small polar molecules after subconjunctival injection. In the microscopy study, which has better resolution and sensitivity of detecting the nanoparticles in the ocular tissues than whole-body imaging, the microscopy results show longer retention of the pRNA nanoparticles in the cells than those suggested by the whole-body imaging. From the microscopy images, although the numbers of cells with internalized pRNA nanoparticles were observed to decrease after the injection, the nanoparticles were retained in a significant number of cells in the eyes even at 20 h after the injection.

Ocular clearance is related to the sizes of the drugs or drug delivery systems. The dsRNA in the present study has 32 nt with molecular weight (MW) of 11 kDa and hydrodynamic diameter of approximately 6 nm. pRNA-3WJ and pRNA-X have 54 nt and MW of 18 kDa and 68 nt and MW of 22 kDa, respectively, which correspond to nanoparticle sizes of approximately 8–12 nm. Although the effects of nanoparticle sizes on ocular clearance after subconjunctival injection have been previously investigated, these studies were performed using synthetic nanoparticles larger than those examined in the present study. In addition, the relationships between nanoparticle sizes and ocular pharmacokinetics are not well defined. In the previous studies, large polystyrene particles of 200 nm and 2 μm were found to remain in the subconjunctival space for up to 2 months and could not penetrate the sclera, and small nanoparticles of 20 nm could diffuse across the sclera and choroid with relatively fast clearance from the periocular tissues (34). Approximately 15% of the administered 20 nm nanoparticles were found to remain in the periocular tissues after 1 day (34) with clearance half-life of 5.5 h in the periocular space (35). Similar results of clearance half-life were observed in another study that investigated Gd-labeled albumin clearance using MRI (32). The clearance of pRNA nanoparticles after subconjunctival injection in the present study is consistent with those observed previously considering that the sizes of the pRNA nanoparticles are within the same order of magnitude as albumin (∼10 nm) and slightly smaller than the 20 nm polystyrene nanoparticle in the previous studies. However, a direct comparison of the concentration results in the present and previous studies cannot be performed because the present whole-body imaging method could not distinguish individual ocular tissues from which the fluorescence signals were emitted (i.e., whole eye not

individual tissues) and the microscopy method could only analyze nanoparticles internalized in cells (i.e., excluding nanoparticles in the extracellular space). Both methods did not allow the determination of nanoparticle concentrations in the ocular tissues. Future studies are required to determine the quantitative relationship between ocular clearance and the characteristics of pRNA nanoparticles after subconjunctival administration.

Potential of RNA Nanoparticles in the Treatment of Ocular Diseases

RNA has the characteristics of DNA and can be designed for the treatment of ocular diseases. Examples of RNA technologies currently used in the eye are siRNA and RNA aptamers (36–39). Due to the unstable nature and the lack of penetrating abilities of nucleotide-based molecules after administration, current proposed therapies of RNA molecules usually require high doses (concentrations) of these molecules for therapeutic effects. The pRNA nanoparticles investigated in the present study are stable and can be easily modified to incorporate RNA therapeutics and serve as their carriers to provide targeted delivery to the cells in the eye for nucleotide-based disease treatments. The advantages of these RNA nanoparticles over other nanodelivery systems include the following (9,10). (a) RNA nanoparticles have defined size, structure, and stoichiometry. The unpredictable side effects arising from heterogeneous particles can thus be avoided. (b) Modular design allows self-assembly of engineered RNA fragments. (c) Branched ratchet shape facilitates vascular penetration and enhanced permeability retention (EPR) effects. (d) Nanoscale size: RNA nanoparticles are large enough to avoid excretion through the urine or a normal blood vessel, yet small enough for receptor-mediated endocytosis (40). (e) Thermodynamically stable, such that the entire construct will not dissociate at ultra-low concentrations in the body. (f) Chemically stable in the blood and resistant to RNase degradation while retaining correct folding and biological functions (10–12). (g) Systemic injection in mice revealed that RNA nanoparticles remain intact and strongly bind to cancers without entering any vital organs (10–12). (h) Display favorable pharmacological profiles in mice; are non-toxic; and do not induce interferon, cytokine production or host immune responses in mice (41). (i) Multivalent nature allows conjugation of several targeting and/or therapeutics for achieving synergistic or enhanced effects (10–12). (j) Economic industrial scale production is possible in a cell-free system. (k) Highly soluble and not prone to aggregation. (l) Polyanionic nature of RNA can avoid nonspecific cell entry since it is unfavorable for RNA to cross the negatively charged cell membranes (42–45). (m) RNA nanoparticles do not contain protein and do not induce host-antibody responses, which will allow repeated treatments over time. (n) RNA is a chemical reagent; therefore, the regulatory process of drug approval is expected to be more favorable compared to protein-based clinical reagents (8,9).

The present study is the first to provide insights into the ocular distribution of pRNA nanoparticles after subconjunctival injection. As expected, topical administration of the pRNA nanoparticles did not provide effective cell internalization in the ocular tissues such as cornea and sclera under the present conditions. With subconjunctival injection, pRNA-X was delivered to the cells of the retina. The delivery of nanoparticles to the retina for cell internalization *via* the subconjunctival route is significant. This result suggests that pRNA-X can be used to deliver drugs such as siRNA and oligonucleotides to the retina for the

treatments of retinal diseases such as neovascularization (4), diabetic macular edema/diabetic retinopathy (46), and viral infection (39), and for neuroprotection (37). In addition, both pRNA-X and pRNA-3WJ could deliver drugs to the cells of the cornea. This approach can be used to deliver nucleotide-based drugs to treat corneal diseases such as corneal neovascularization (36) and dystrophies (38). However, the pRNA nanoparticles are prone to fast ocular clearance after subconjunctival injection under the conditions in the present study. The delivery of the pRNA nanoparticles *via* subconjunctival injection for long term therapeutic effects will likely require the development of a sustained-release drug delivery system for the nanoparticles.

Conclusions

The distribution and clearance of pRNA nanoparticles derived from the 3WJ of pRNA of bacteriophage phi29 DNA packaging motor were investigated for ocular delivery in mice after subconjunctival injection *in vivo*. Both pRNA-X and pRNA-3WJ were found in the cells of the conjunctiva, cornea, and sclera after the injection, but only pRNA-X was found in the cells of the retina. The different ocular distributions of the pRNA nanoparticles are probably related to the sizes and shapes of the nanoparticles. In general, ocular clearance of the pRNA nanoparticles was relatively fast after the injection, which is consistent with previous subconjunctival studies of small molecules and macromolecules. Lymphatic clearance through the cervical lymph node was an important route of clearance for the nanoparticles after subconjunctival injection. Topical administration of eyedrops was not effective in delivering the nanoparticles to the cells in ocular tissues. The present study demonstrated that subconjunctival injection of pRNA nanoparticles could deliver the nanoparticles to the cells of the cornea and retina. This method has the potential to deliver nucleotide-based drugs to these tissues for the treatment of ocular diseases.

Acknowledgments

Acknowledgments and Disclosures: This paper is dedicated to Dr. Stephen J. Ryan, the founder of the Arnold and Mabel Beckman Initiative for Macular Research. The research was supported in part by NCI Cancer Nanotechnology Platform Partnership Program: *RNA Nanotechnology for Cancer Therapy*, as the NIH U01 CA151648 program directed by Peixuan Guo; and Beckman Initiative for Macular Research Grant 1108 (to Peixuan Guo) as well as 1210 (to David Gamm and Dan Shu). The content is solely the responsibility of the authors and does not necessarily represent the official views of NIH. Funding to P. Guo's Endowed Chair in Nanobiotechnology position is by the William Fairish Endowment Fund. P. Guo is a co-founder of Kylin Therapeutics, Inc., and Biomotor and Nucleic Acid Nano-technology Development Corp. Ltd.. The authors thank Drs. Winston W-Y. Kao and Ying Xia for providing the AxioCam Observer Z1 microscopes in the study; Dr. Jinsong Hao for her technical support; and Dr. Jiukuan Hao for helpful discussion. The authors also thank Drs. Maria B. Grant for collaboration and discussion; David Gamm, Michael Boulton, and Mark Humayun for constructive comments and inspiring discussion.

References

1. Fattal E, Bochot A. Ocular delivery of nucleic acids: antisense oligonucleotides, aptamers and siRNA. Adv Drug Deliv Rev. 2006; 58:1203–23. [PubMed: 17097190]
2. Pieramici DJ, Rabena MD. Anti-VEGF therapy: comparison of current and future agents. Eye (Lond). 2008; 22:1330–6. [PubMed: 18497829]
3. de Smet MD, Meenken CJ, van den Horn GJ. Fomivirsen—a phosphorothioate oligonucleotide for the treatment of CMV retinitis. Ocul Immunol Inflamm. 1999; 7:189–98. [PubMed: 10611727]

4. Ng EW, Shima DT, Calias P, Cunningham ET Jr, Guyer DR, Adamis AP. Pegaptanib, a targeted anti-VEGF aptamer for ocular vascular disease. Nat Rev Drug Discov. 2006; 5:123–32. [PubMed: 16518379]
5. FDA. A safety and efficacy study of E10030 (anti-PDGF pegylated aptamer) plus Lucentis for neovascular age-related macular degeneration. 2012. Clinicaltrials.govNCT01089517
6. Lee SS, Robinson MR. Novel drug delivery systems for retinal diseases. A review. Ophthalmic Res. 2009; 41:124–35. [PubMed: 19321933]
7. Guo P, Zhang C, Chen C, Garver K, Trottier M. Inter-RNA interaction of phage phi29 pRNA to form a hexameric complex for viral DNA transportation. Mol Cell. 1998; 2:149–55. [PubMed: 9702202]
8. Guo P. The emerging field of RNA nanotechnology. Nat Nanotechnol. 2010; 5:833–42. [PubMed: 21102465]
9. Guo P, Haque F, Hallahan B, Reif R, Li H. Uniqueness, advantages, challenges, solutions, and perspectives in therapeutics applying RNA nanotechnology. Nucleic Acid Ther. 2012; 22:226–45. [PubMed: 22913595]
10. Haque F, Shu D, Shu Y, Shlyakhtenko LS, Rychahou PG, Evers BM, et al. Ultrastable synergistic tetravalent RNA nanoparticles for targeting to cancers. Nano Today. 2012; 7:245–57. [PubMed: 23024702]
11. Liu J, Guo S, Cinier M, Shlyakhtenko LS, Shu Y, Chen C, et al. Fabrication of stable and RNase-resistant RNA nanoparticles active in gearing the nanomotors for viral DNA packaging. ACS Nano. 2011; 5:237–46. [PubMed: 21155596]
12. Shu D, Shu Y, Haque F, Abdelmawla S, Guo P. Thermodynamically stable RNA three-way junction for constructing multifunctional nanoparticles for delivery of therapeutics. Nat Nanotechnol. 2011; 6:658–67. [PubMed: 21909084]
13. Macha S, Mitra AK. Ocular pharmacokinetics in rabbits using a novel dual probe microdialysis technique. Exp Eye Res. 2001; 72:289–99. [PubMed: 11180978]
14. Berezovsky DE, Patel SR, McCarey BE, Edelhauser HF. In vivo ocular fluorophotometry: delivery of fluoresceinated dextrans via transscleral diffusion in rabbits. Invest Ophthalmol Vis Sci. 2011; 52:7038–45. [PubMed: 21791594]
15. Li SK, Lizak MJ, Jeong EK. MRI in ocular drug delivery. NMR Biomed. 2008; 21:941–56. [PubMed: 18186077]
16. Kim SH, Lutz RJ, Wang NS, Robinson MR. Transport barriers in transscleral drug delivery for retinal diseases. Ophthalmic Res. 2007; 39:244–54. [PubMed: 17851264]
17. Urtti A. Challenges and obstacles of ocular pharmacokinetics and drug delivery. Adv Drug Deliv Rev. 2006; 58:1131–5. [PubMed: 17097758]
18. Gaudana R, Jwala J, Boddu SH, Mitra AK. Recent perspectives in ocular drug delivery. Pharm Res. 2009; 26:1197–216. [PubMed: 18758924]
19. Maurice D. Review: practical issues in intravitreal drug delivery. J Ocul Pharmacol Ther. 2001; 17:393–401. [PubMed: 11572470]
20. Dastjerdi MH, Sadrai Z, Saban DR, Zhang Q, Dana R. Corneal penetration of topical and subconjunctival bevacizumab. Invest Ophthalmol Vis Sci. 2011; 52:8718–23. [PubMed: 22003112]
21. Bejjani RA, BenEzra D, Cohen H, Rieger J, Andrieu C, Jeanny JC, et al. Nanoparticles for gene delivery to retinal pigment epithelial cells. Mol Vis. 2005; 11:124–32. [PubMed: 15735602]
22. Bourges JL, Gautier SE, Delie F, Bejjani RA, Jeanny JC, Gurny R, et al. Ocular drug delivery targeting the retina and retinal pigment epithelium using polylactide nanoparticles. Invest Ophthalmol Vis Sci. 2003; 44:3562–9. [PubMed: 12882808]
23. Andrieu-Soler C, Halhal M, Boatright JH, Padove SA, Nickerson JM, Stodulkova E, et al. Single-stranded oligonucleotide-mediated in vivo gene repair in the rd1 retina. Mol Vis. 2007; 13:692–706. [PubMed: 17563719]
24. Chopra P, Hao J, Li SK. Iontophoretic transport of charged macromolecules across human sclera. Int J Pharm. 2010; 388:107–13. [PubMed: 20045044]
25. Wen H, Hao J, Li SK. Characterization of human sclera barrier properties for transscleral delivery of bevacizumab and ranibizumab. J Pharm Sci. 2013; 102:892–903. [PubMed: 23212655]

26. Demetriades AM, Deering T, Liu H, Lu L, Gehlbach P, Packer JD, et al. Trans-scleral delivery of antiangiogenic proteins. J Ocul Pharmacol Ther. 2008; 24:70–9. [PubMed: 18370877]
27. Amaral J, Fariss RN, Campos MM, Robison WG Jr, Kim H, Lutz R, et al. Transscleral-RPE permeability of PEDF and ovalbumin proteins: implications for subconjunctival protein delivery. Invest Ophthalmol Vis Sci. 2005; 46:4383–92. [PubMed: 16303924]
28. Kim SH, Galban CJ, Lutz RJ, Dedrick RL, Csaky KG, Lizak MJ, et al. Assessment of subconjunctival and intrascleral drug delivery to the posterior segment using dynamic contrast-enhanced magnetic resonance imaging. Invest Ophthalmol Vis Sci. 2007; 48:808–14. [PubMed: 17251481]
29. Lee SJ, He W, Robinson SB, Robinson MR, Csaky KG, Kim H. Evaluation of clearance mechanisms with transscleral drug delivery. Invest Ophthalmol Vis Sci. 2010; 51:5205–12. [PubMed: 20484583]
30. Li SK, Molokhia SA, Jeong EK. Assessment of subconjunctival delivery with model ionic permeants and magnetic resonance imaging. Pharm Res. 2004; 21:2175–84. [PubMed: 15648248]
31. Lee TW, Robinson JR. Drug delivery to the posterior segment of the eye II: development and validation of a simple pharmacokinetic model for subconjunctival injection. J Ocul Pharmacol Ther. 2004; 20:43–53. [PubMed: 15006158]
32. Kim SH, Csaky KG, Wang NS, Lutz RJ. Drug elimination kinetics following subconjunctival injection using dynamic contrast-enhanced magnetic resonance imaging. Pharm Res. 2008; 25:512–20. [PubMed: 17674155]
33. Kim H, Robinson MR, Lizak MJ, Tansey G, Lutz RJ, Yuan P, et al. Controlled drug release from an ocular implant: an evaluation using dynamic three-dimensional magnetic resonance imaging. Invest Ophthalmol Vis Sci. 2004; 45:2722–31. [PubMed: 15277497]
34. Amrite AC, Kompella UB. Size-dependent disposition of nanoparticles and microparticles following subconjunctival administration. J Pharm Pharmacol. 2005; 57:1555–63. [PubMed: 16354399]
35. Amrite AC, Edelhauser HF, Singh SR, Kompella UB. Effect of circulation on the disposition and ocular tissue distribution of 20 nm nanoparticles after periocular administration. Mol Vis. 2008; 14:150–60. [PubMed: 18334929]
36. Chang JH, Garg NK, Lunde E, Han KY, Jain S, Azar DT. Corneal neovascularization: an anti-VEGF therapy review. Surv Ophthalmol. 2012; 57:415–29. [PubMed: 22898649]
37. Ishikawa S, Hirata A, Nakabayashi J, Iwakiri R, Okinami S. Neuroprotective effect of small interfering RNA targeted to caspase-3 on rat retinal ganglion cell loss induced by ischemia and reperfusion injury. Curr Eye Res. 2012; 37:907–13. [PubMed: 22642649]
38. Williams KA, Klebe S. Gene therapy for corneal dystrophies and disease, where are we? Curr Opin Ophthalmol. 2012; 23:276–9. [PubMed: 22543480]
39. Henry SP, Miner RC, Drew WL, Fitchett J, York-Defalco C, Rapp LM, et al. Antiviral activity and ocular kinetics of antisense oligonucleotides designed to inhibit CMV replication. Invest Ophthalmol Vis Sci. 2001; 42:2646–51. [PubMed: 11581212]
40. Li W, Szoka FC Jr. Lipid-based nanoparticles for nucleic acid delivery. Pharm Res. 2007; 24:438–49. [PubMed: 17252188]
41. Abdelmawla S, Guo S, Zhang L, Pulukuri SM, Patankar P, Conley P, et al. Pharmacological characterization of chemically synthesized monomeric phi29 pRNA nanoparticles for systemic delivery. Mol Ther. 2011; 19:1312–22. [PubMed: 21468004]
42. de Fougerolles A, Vornlocher HP, Maraganore J, Lieberman J. Interfering with disease: a progress report on siRNA-based therapeutics. Nat Rev Drug Discov. 2007; 6:443–53. [PubMed: 17541417]
43. Kim DH, Rossi JJ. Strategies for silencing human disease using RNA interference. Nat Rev Genet. 2007; 8:173–84. [PubMed: 17304245]
44. Seth S, Johns R, Templin MV. Delivery and biodistribution of siRNA for cancer therapy: challenges and future prospects. Ther Deliv. 2012; 3:245–61. [PubMed: 22834200]
45. Rozema DB, Lewis DL, Wakefield DH, Wong SC, Klein JJ, Roesch PL, et al. Dynamic PolyConjugates for targeted in vivo delivery of siRNA to hepatocytes. Proc Natl Acad Sci U S A. 2007; 104:12982–7. [PubMed: 17652171]

46. Nguyen QD, Schachar RA, Nduaka CI, Sperling M, Basile AS, Klamerus KJ, et al. Dose-ranging evaluation of intravitreal siRNA PF-04523655 for diabetic macular edema (the DEGAS study). Invest Ophthalmol Vis Sci. 2012; 53:7666–74. [PubMed: 23074206]

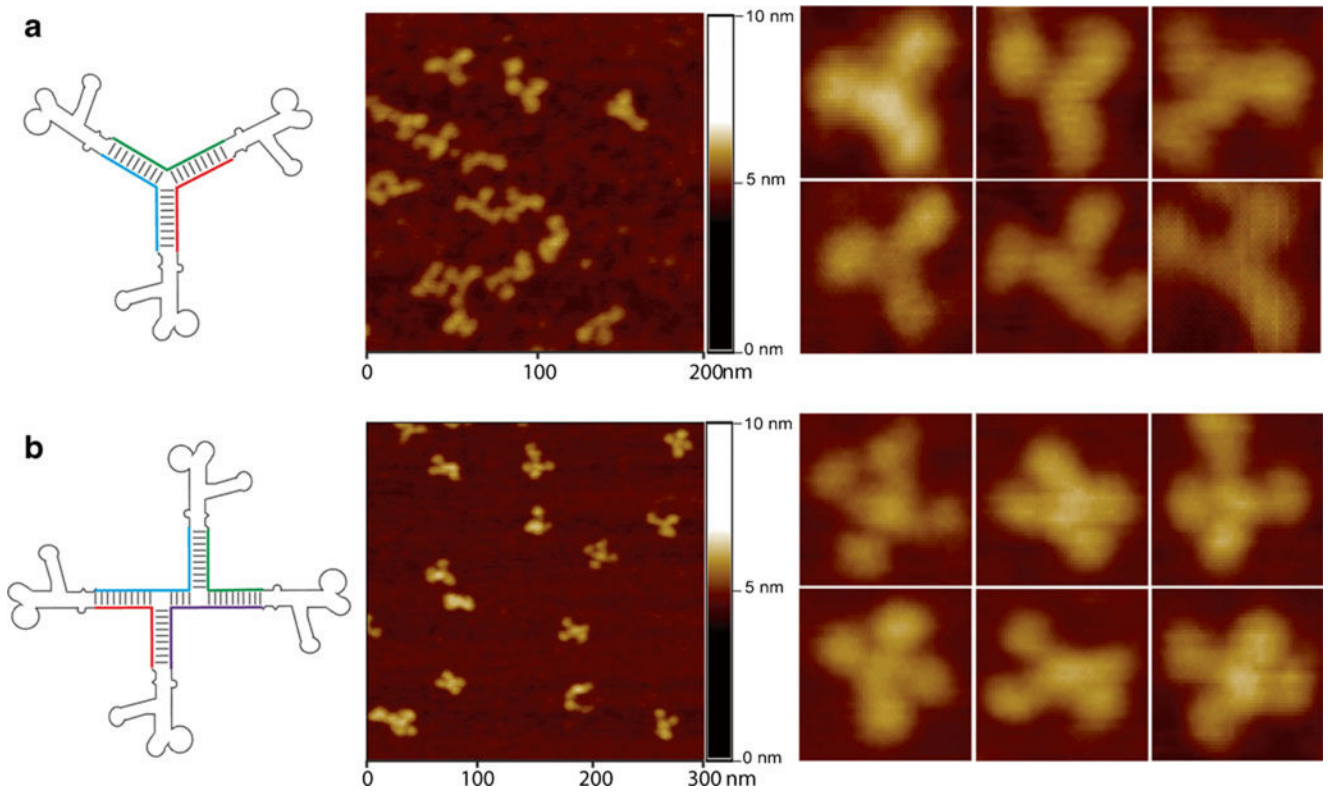

Fig. 1.

Construction of (**a**) trivalent RNA nanoparticle consisting of three pRNA molecules bound at the pRNA-3WJ core (pRNA-3WJ) and (**b**) the extension to tetravalent RNA nanoparticles of X shape (pRNA-X) and their corresponding atomic force microscopy (AFM) images (10,12), respectively.

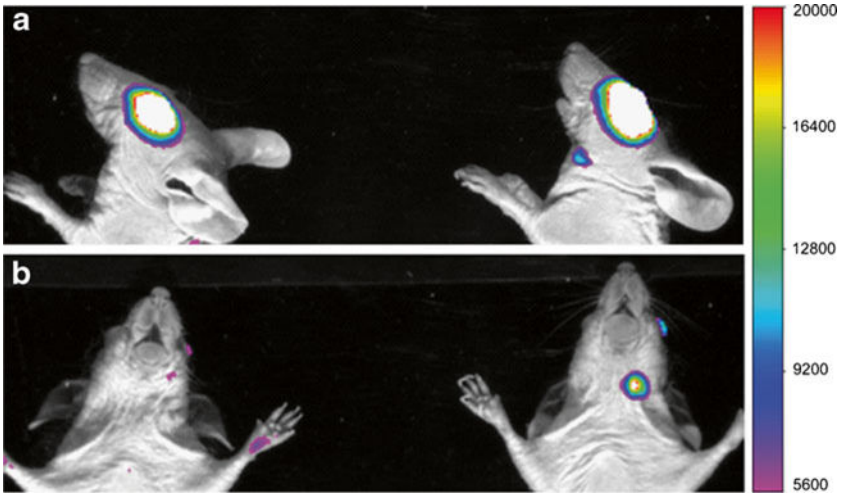

Fig. 2.

Representative fluorescence images of the whole body (*upper body*) at 2 h after subconjunctival injection of Alexa647 (*left mouse*) and pRNA-X (*right mouse*) in whole-body imaging. (**a**) Side lying position; (**b**) prone position. The *white color* represents high fluorescence intensity beyond the scale.

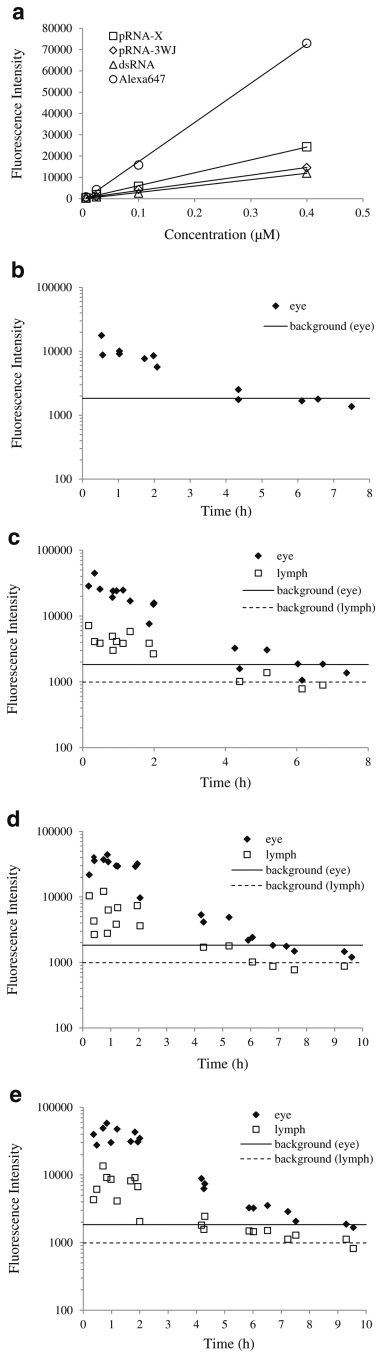

Fig. 3.

(**a**) Fluorescence intensity vs. concentration of Alexa647, dsRNA, pRNA-3WJ, and pRNA-X in PBS in vials. (**b** to **e**) Mean fluorescence intensities at the eyes (diamonds) and the cervical lymph nodes (squares) after subconjunctival injection. (**b**) Alexa647; (**c**) dsRNA; (**d**) pRNA-3WJ; (**e**) pRNA-X. The background fluorescence levels at the eyes (solid lines) and lymph nodes (dotted lines) were obtained from animals without the injection (control). Individual data points obtained from three animals are presented in each plot.

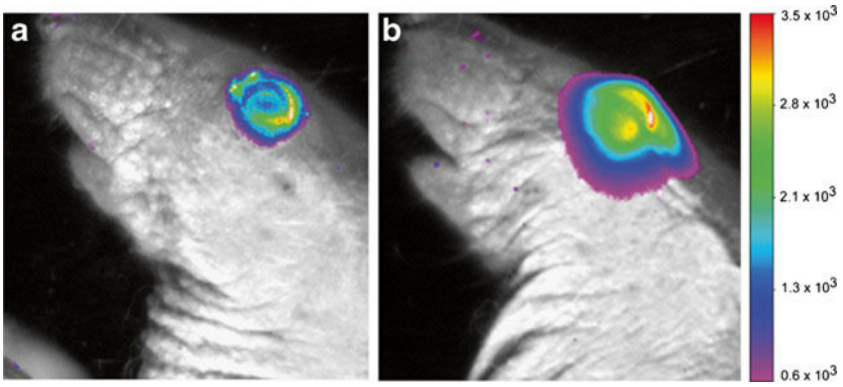

Fig. 4.

Representative ocular fluorescence images of the eye after subconjunctival injection of pRNA-X in whole-body imaging. (**a**) 2 h time point; (**b**) 4 h time point after the injection. The *white color* represents high fluorescence intensity beyond the scale.

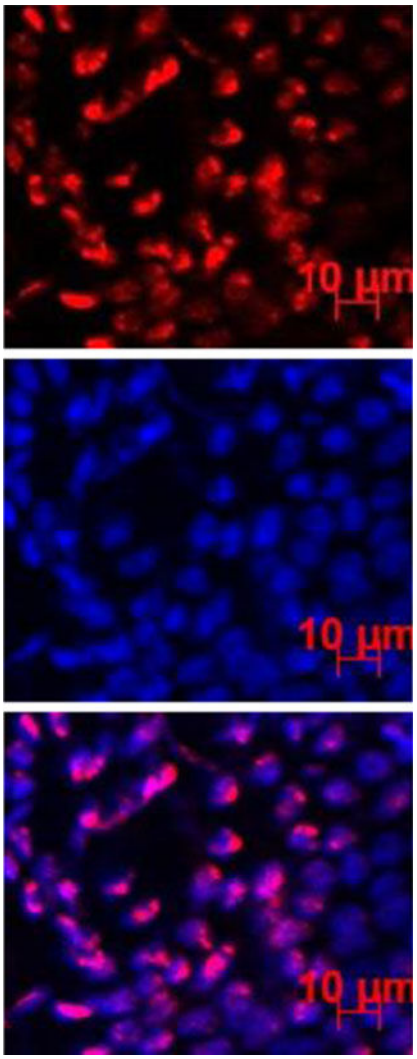

Fig. 5.

Representative fluorescence images of the conjunctiva at 6 h after subconjunctival injection of pRNA-X. *Blue color* represents the cell nucleus stained by DAPI; *red color* represents the Alexa647-labeled nanoparticles.

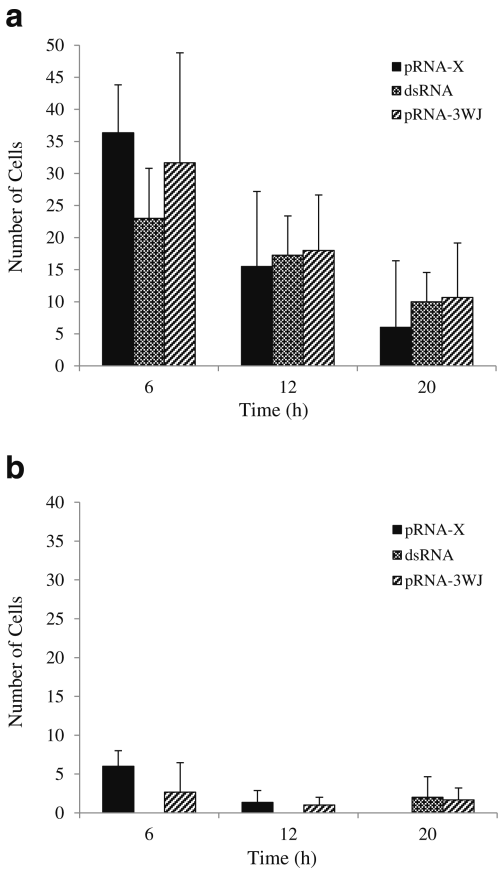

Fig. 6.

Numbers of cells with pRNA and dsRNA internalization in the conjunctiva after subconjunctival injection. (**a**) Superior conjunctiva (near the injection site); (**b**) Inferior conjunctiva. Mean ± SD (*n* = 3–4).

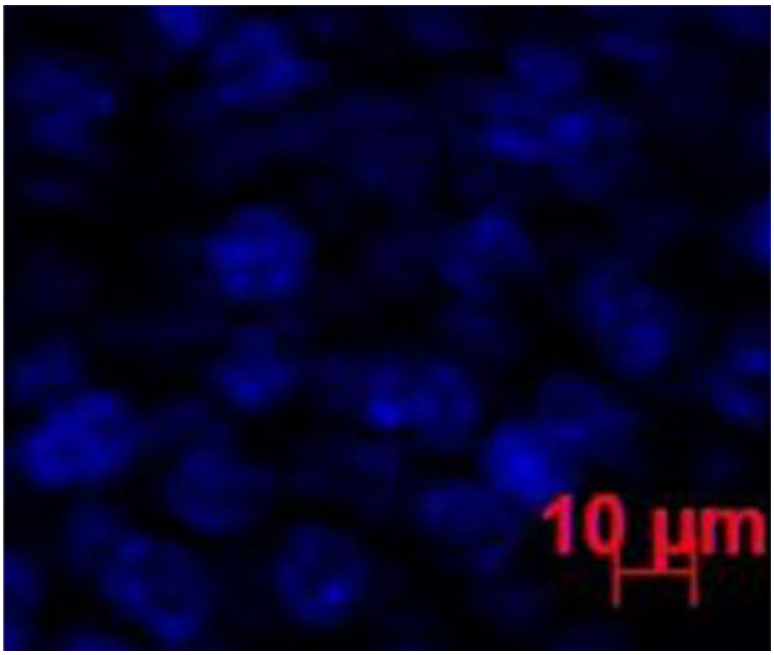

Fig. 7.

Representative fluorescence image of the cornea at 6 h after subconjunctival injection of Alexa647. *Blue color* represents the cell nucleus stained by DAPI. No *red color* that represents the Alexa647 marker could be found in the image.

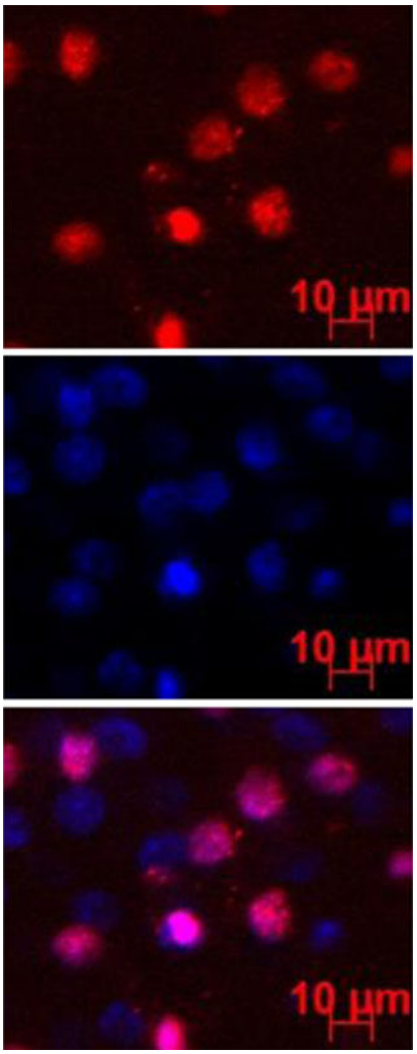

Fig. 8.

Representative fluorescence images of the endothelial cells in the cornea at 6 h after subconjunctival injection of pRNA-X. *Blue color* represents the cell nucleus stained by DAPI; *red color* represents the Alexa647-labeled nanoparticles.

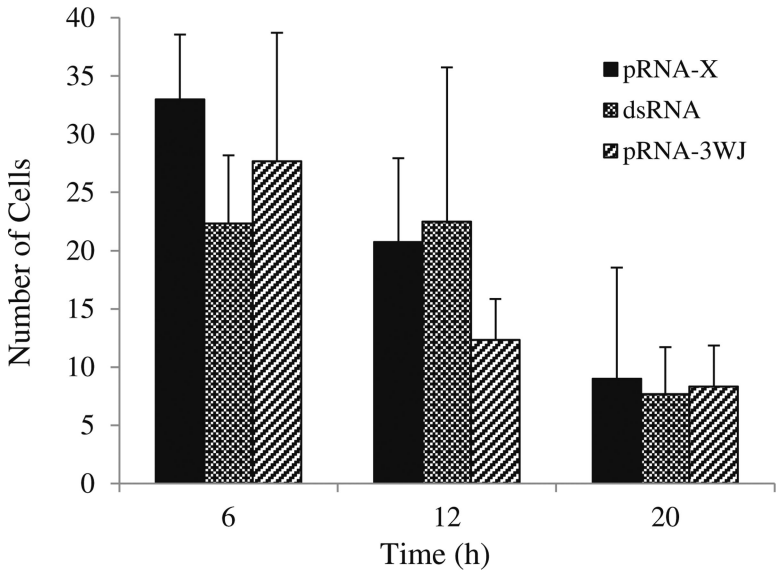

Fig. 9.

Numbers of cells with pRNA and dsRNA internalization in the cornea after subconjunctival injection. Mean ± SD (*n* = 3–4).

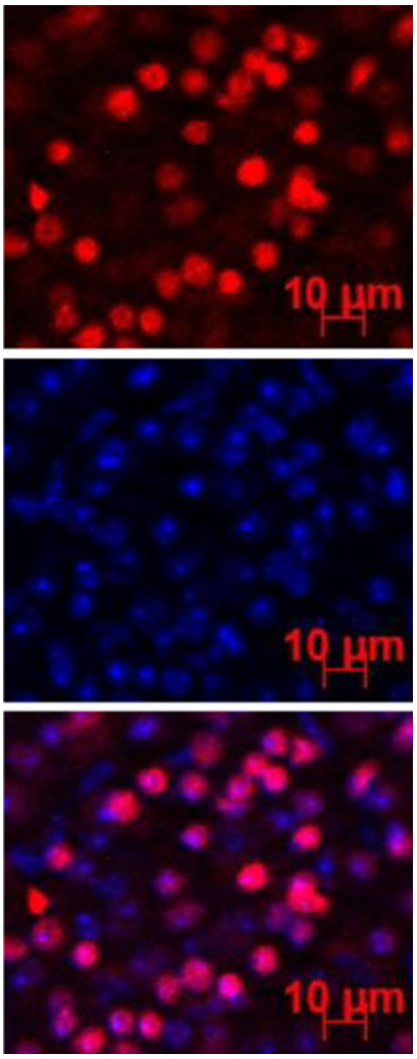

Fig. 10.

Representative fluorescence images of the retina at 6 h after subconjunctival injection of pRNA-X. *Blue color* represents the cell nucleus stained by DAPI; *red color* represents the Alexa647-labeled nanoparticles.

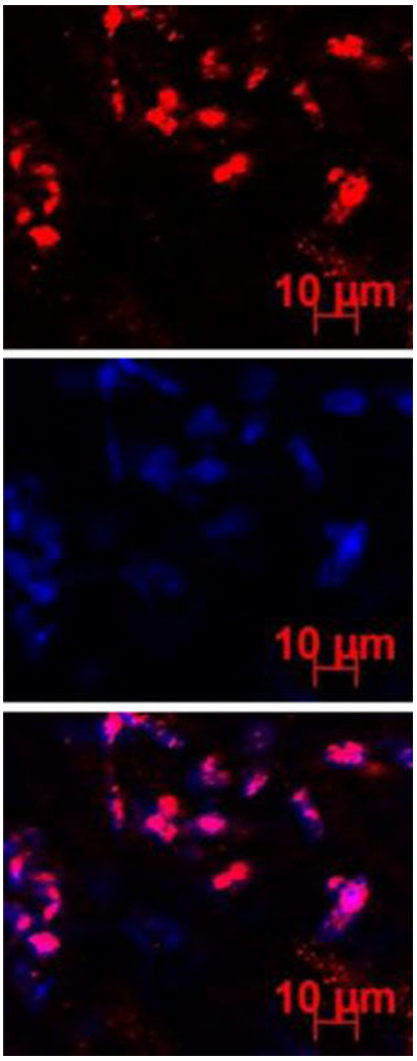

Fig. 11.

Representative fluorescence images of the sclera at 6 h after subconjunctival injection of pRNA-X. *Blue color* represents the cell nucleus stained by DAPI; *red color* represents the Alexa647-labeled nanoparticles.

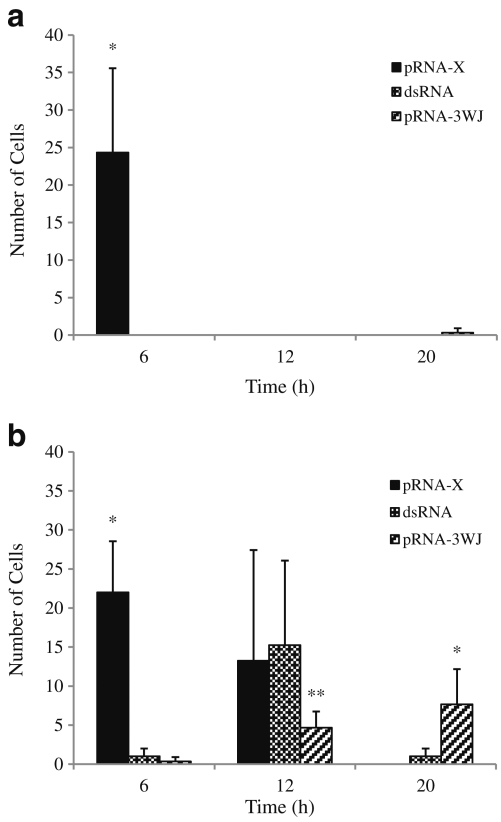

Fig. 12.

Numbers of cells with pRNA and dsRNA internalization in the retina and sclera after subconjunctival injection. (**a**) Retina; (**b**) Sclera. Mean ± SD (n = 3–4). * indicates the group is statistically higher than the other two groups at the time point; ** indicates the group is statistically lower than the other two groups at the time point.